



A Novel Method for Testing and Evaluating the Fatigue Life of Metal Vibration Absorber

Y. Peng¹ · D. Jia¹ · Z. Chen¹ · Y. Gao¹ · W. Zhong^{1,2}

Received: 3 July 2023 / Accepted: 9 May 2024
© The Society for Experimental Mechanics, Inc 2024

Abstract

Metal vibration absorber has been widely used to reduce the structural vibration under various complex environmental conditions, the fatigue reliability of which has an important influence on the safety of the structure. In this paper, a novel fatigue failure criterion when the residual preload displacement of metal vibration absorber is equal to the fatigue displacement amplitude is proposed to determine the fatigue life of metal vibration absorber. And a set of fatigue failure life prediction method is developed to obtain the failure life of non-failed metal vibration absorber. The predicted load versus life ($P-N$) curve of the metal vibration absorber under different load levels shows a good power function relation. Based on the fatigue displacement amplitude-life curves and the residual preload displacement-life curves of the metal vibration absorbers, a fatigue failure assessment diagram is successfully established. Further, the residual fatigue failure life of in-service metal vibration absorber can also be predicted according to the failure assessment diagram. By means of the scanning electron microscopy and the three-dimensional tomography equipment, the microanalyses of metal wire components after fatigue tests are conducted, and the fatigue wear and fracture law of metal wire in the metal vibration absorber is mastered.

Keywords Metal vibration absorber · Failure criterion · $P-N$ curve · Failure assessment diagram · Microanalysis · Safety assessment

Introduction

In order to ensure the lasting reliability of key structures, it is necessary to perform vibration reduction design in aerospace, ships and other major engineering fields. Metal vibration absorber has not only the inherent characteristic of the selected metal material, but also the elastic and damping characteristics similar to rubber. It can reduce the structural vibration through the dry friction of artificially wound metal wire components, and its shape can be customized according to different service environments. Therefore, it has been widely used to reduce the structural vibration

under various complex environmental conditions [1–4] because of its designable stiffness, high and low temperature resistance, and ageing resistance etc. Research on the metal vibration absorbers originated in the United States in 1950s [5, 6]. After years of development, the manufacturing technique of metal vibration absorber has been relatively mature, which can be mainly divided into 6 steps [7]: wire material selection, wire winding, wire tension, blank weaving, cold pressing forming and post-treatment. The mainly control parameters involve wire material [8–10], wire diameter [11], cross-section shape [12], braiding method [13], forming pressure [14] etc. The change of each parameter will lead to the different performance of metal vibration absorber. Therefore, the dispersibility of metal vibration absorber is general larger than the traditional metal material. Zhang et al. [15] conducted a CT scan on the internal microstructure of metal vibration absorbers. It can be seen that there are three typical contact states (separation, slip and adhesion) among different parts of the metal wire component [16, 17], and the vibration damping performance of the metal vibration absorber is mainly achieved through the

✉ W. Zhong
zhongwz@caep.cn

¹ Institute of Systems Engineering, China Academy of Engineering Physics, 621999 Mianyang, Sichuan, China

² Vibration and Vibration of Engineering Materials and Structures Key Laboratory of Sichuan Province, 621999 Mianyang, Sichuan, China

slip state. Because metal vibration absorber is usually suffered alternating fatigue load in actual service environment, it is of great significance to study the fatigue performance of the metal vibration absorber. Jiang et al. [18, 19]. performed the fatigue experiments of metal vibration absorbers. The results indicate that the fatigue life will increase when the metal wire diameter, prestress and relative density of the metal vibration absorbers increase. Li [20] carried out sinusoidal constant-frequency fatigue tests of metal vibration absorbers. The change law between inherent frequency of vibration absorber and fatigue life is obtained. Then, the fatigue failure life of the metal vibration absorber is successfully determined according to the failure criterion of inherent frequency variation of 10%. However, this method requires extra resonance frequency test to obtain the real-time inherent frequency of metal vibration absorber, and the fatigue test must be interrupted several times. In addition, the fatigue failure life of the metal vibration absorber will be affected to some extent during the resonance frequency test. Cao et al. [21]. proposed a coupling damage factor of stiffness and damping as the failure criterion to determine the fatigue failure life of metal vibration absorber, but the effectiveness needs to be further verified. Therefore, although some researchers have carried out fatigue research on the metal vibration absorbers, the current research results are not mature and have not been recognized by everyone.

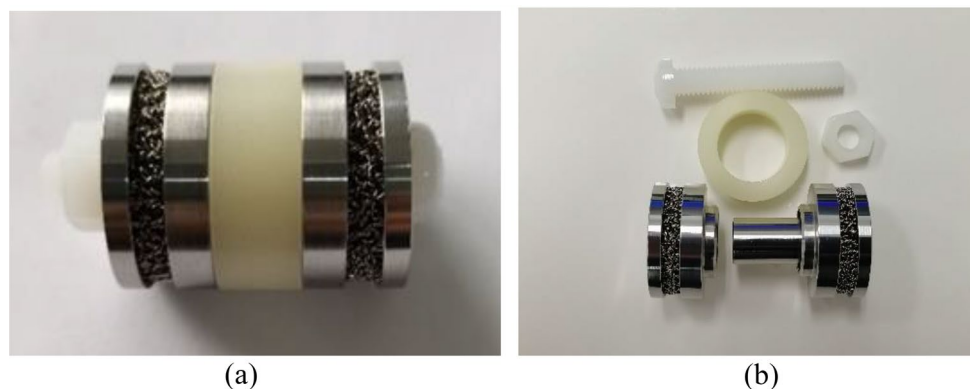
In this paper, the axial high-cycle fatigue experiment of the metal vibration absorber is conducted. Based on the fatigue displacement amplitude and residual preload displacement of the metal vibration absorber, a new fatigue failure criterion is put forward. Further, the fatigue failure life of the metal vibration absorber can be determined. In addition, a fatigue failure assessment diagram is successfully established on the basis of the displacement amplitude versus life curves and the residual preload displacement versus life curves of metal vibration absorbers, which can be used to assess the residual fatigue life of in-service metal vibration absorber. Finally, in order to research the microscopic fatigue failure behaviors, the microcosmic wear and fracture of metal wires in metal vibration absorbers are

analyzed by the scanning electron microscopy (SEM) and three-dimensional tomography (μ CT) devices.

Experimental Conditions

The configuration of the metal vibration absorber adopted in this study is shown in Fig. 1, which is suitable for the situation where axial fatigue load is mainly suffered in the service environment. The axial direction of vibration absorber is connected using a bolt with the diameter of 6 mm. The thickness of the mounting plate in the middle of the vibration absorber is 8 mm. The material of metal wire is 1Cr18Ni9Ti, and the diameter of the metal wire is 0.3 mm. Since the vibration absorption function of metal vibration absorber is mainly depended on the metal wire component at both ends, therefore, the metal wire component is the core part of the whole vibration absorber. The high-cycle fatigue test of vibration absorber is conducted by the high frequency electromagnetic fatigue testing machine with maximum load of 1 kN and maximum test frequency of 200 Hz. As the metal vibration absorber is a non-standard structure, in order to connect the vibration absorber to the testing machine, special transition connection fixture needs to be designed, as shown in Fig. 2. In order to reflect the fatigue loosening phenomenon that may occur in the actual use of the metal vibration absorber, the whole metal vibration absorber is adopted to carry out the fatigue test. The upper fatigue loading fixture adopts hollow design. It is easy to tighten the sample through hex bolts. The upper and lower fixtures are fastened on the test machine through the drill chuck of the testing machine.

Fig. 1 Picture of the metal vibration absorber (a) entire state (b) split state



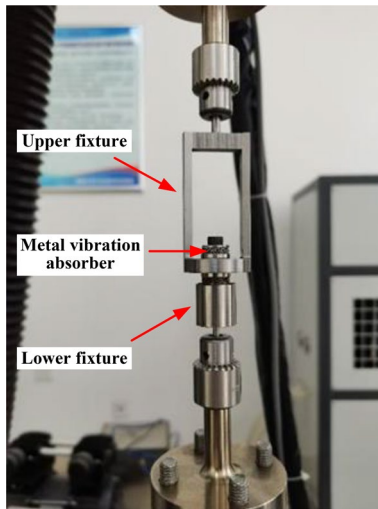


Fig. 2 Axial loading fixture of high-cycle fatigue test of the metal vibration absorber

High Cycle Fatigue Test of the Metal Vibration Absorber

Analysis of the Fatigue Testing Result

The central metal hollow cylinder has a limiting action (see Fig. 1). There is an initial interval between the leftmost metal plate and the central metal hollow cylinder in the natural state. And the interval will close in the preload state. Therefore, the initial preload displacement can be determined according to the initial interval of metal vibration absorber in the natural state. Table 1 lists the testing results of the initial preload displacements of the metal vibration absorbers. It can be observed that the initial preload displacements of

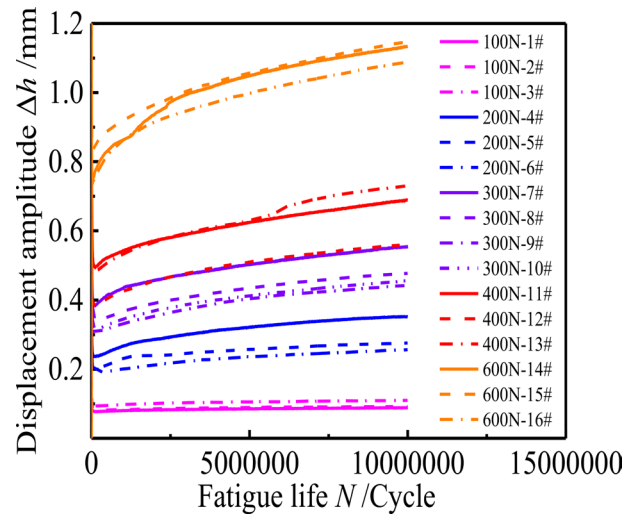


Fig. 3 Displacement amplitude versus fatigue life curves of the metal vibration absorbers under different fatigue load levels

the metal vibration absorbers have some dispersity, ranging from 1.410 mm to 1.635 mm. Because the initial state of the metal vibration absorber is pre-lock state, the initial pre-load displacement is measured after the preload is removed. However, some metal vibration absorbers recover well, while the others may have a large permanent deformation when the preload is removed, which cause the dispersity of the initial preload displacement measurement of the metal vibration absorber.

Figure 3 shows the relations of the fatigue displacement amplitude versus fatigue life of 16 metal vibration absorbers. The results indicate that the initial displacement amplitude of each vibration absorber has a rapid decline stage, and the minimum displacement amplitude will occur at about 0.1 million of fatigue life. Then the displacement amplitude

Table 1 Initial preload displacement measurements of the metal vibration absorbers

specimen number	Maximum load P_{max} / N	Height 1 H_1 / mm	Height 2 H_2 / mm	Average height H / mm	Preload height H_1 / mm	Initial preload displacement δ_i / mm
100 N-50 Hz-1#	100	27.62	27.59	27.605	25.97	1.635
100 N-50 Hz-2#	100	27.65	27.63	27.640	26.02	1.620
100-50 Hz-3#	100	27.54	27.44	27.490	26.02	1.470
200-50 Hz-4#	200	27.42	27.45	27.435	26.02	1.415
200-50 Hz-5#	200	27.46	27.45	27.455	26.01	1.445
200-50 Hz-6#	200	27.65	27.63	27.640	26.03	1.610
300 N-50HZ-7#	300	27.46	27.44	27.450	25.98	1.470
300 N-50HZ-8#	300	27.63	27.67	27.650	26.03	1.620
300 N-50HZ-9#	300	27.58	27.57	27.575	26.02	1.555
300 N-50HZ-10#	300	27.57	27.60	27.585	26.02	1.565
400 N-50HZ-11#	400	27.48	27.54	27.510	25.98	1.530
400 N-50HZ-12#	400	27.48	27.51	27.495	26.01	1.485
400 N-50HZ-13#	400	27.53	27.51	27.520	26.02	1.500
600 N-50HZ-14#	600	27.42	27.48	27.450	26.01	1.440
600 N-50HZ-15#	600	27.41	27.43	27.420	26.01	1.410
600 N-50HZ-16#	600	27.62	27.64	27.630	26.02	1.610

increases slowly along with the fatigue life. Under the same load level, the displacement amplitudes of different metal vibration absorbers have a certain dispersion, and it can be observed that there is no obvious consistency between the preload displacement and the fatigue displacement amplitude. Because the larger of the displacement amplitude, the worse of the carrying capacity for metal vibration absorber, and the fatigue failure will occur more easily. Therefore, Figs. 4, 5, 6, 7 and 8 show the evolutions of load-displacement cyclic hysteresis curves of the samples with largest displacement amplitudes at various load levels. It can be observed that the load-displacement hysteresis curves show good shapes when the fatigue life of each vibration absorber is 0.05 million cycles, which indicate that the vibration damping performances are also good. When the maximum fatigue load is 100 N, the load-displacement hysteresis curve of metal vibration absorber changes a little after 10 million cycles of fatigue test. Under different fatigue load levels, the displacement amplitude of each metal vibration absorber does not exceed the initial preload displacement when the fatigue life reaches 10 million cycles. Further analysis shows that the load-displacement hysteresis curve of the metal vibration absorber also has some vibration damping performance when the fatigue load is less than 400 N and the life reaches 10 million cycles. However, the load-displacement hysteresis curve of the vibration absorber almost coincides near the zero load when the maximum fatigue load is 600 N and the fatigue life reaches 10 million cycles, which can be considered that the vibration damping performance has been lost. Consequently, it is unreasonable to adopt the initial preload displacement as the fatigue failure criterion of the metal vibration absorber.

The secant stiffness of the load-displacement hysteresis curve represents the bearing capacity of the metal vibration absorber. The larger the stiffness of vibration absorber is, the stronger the bearing capacity is. The analysis result shows that the maximum secant stiffness S_{\max} of each metal vibration absorber occurs at the position of the smallest initial displacement amplitude, which can be calculated by Eq. (1)

$$S_{\max} = \frac{\Delta P}{\Delta h_{\min}} \quad (1)$$

in which ΔP represents the peak and valley load amplitude, namely $\Delta P = P_{\max} - P_{\min}$, Δh_{\min} is the minimum displacement amplitude in the initial fatigue loading stage. The secant stiffness change rate λ_{10m} after 10 million cycles of fatigue test can be calculated by Eq. (2).

$$\lambda_{10m} = \frac{100(S_{\max} - S_{10m})}{S_{\max}} \quad (2)$$

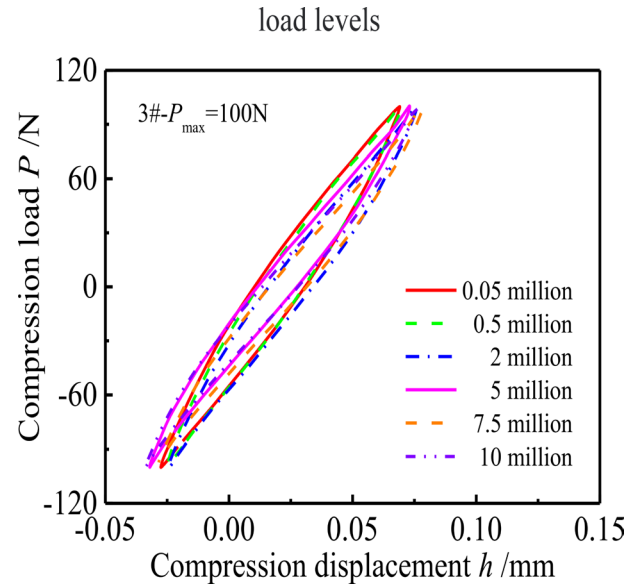


Fig. 4 Compression load-displacement hysteresis curves of 3# specimen under different fatigue lives

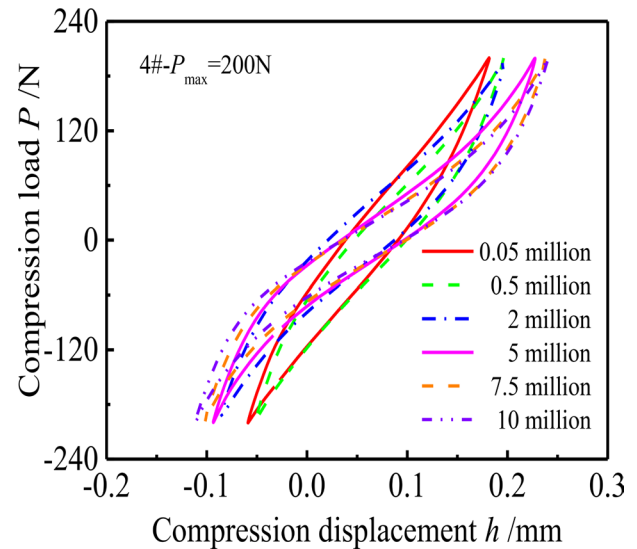


Fig. 5 Compression load-displacement hysteresis curves of 4# specimen under different fatigue lives

where S_{10m} represents the secant stiffness of the metal vibration absorber after 10 million cycles of fatigue test. Table 2 lists the secant stiffness change rates of the 16 metal vibration absorbers. The results indicate that the stiffness change rates of the metal vibration absorbers after 10 million cycles of fatigue tests have no obvious law under different fatigue load levels. Therefore, the fatigue failure life of metal vibration absorber cannot be judged by the secant stiffness change rate.

Since there is an inversely proportional relationship between the fatigue displacement amplitude of metal vibration absorber and the residual preload displacement, it is

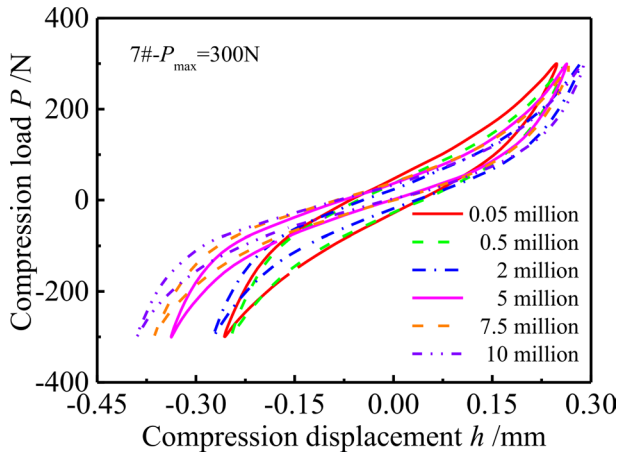


Fig. 6 Compression load-displacement hysteresis curves of 7# specimen under different fatigue lives

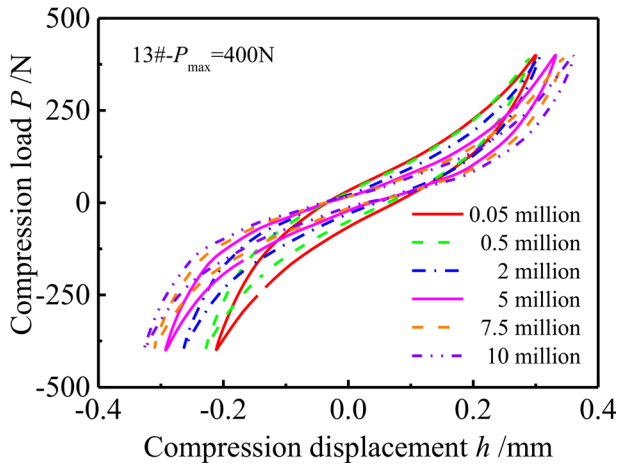


Fig. 7 Compression load-displacement hysteresis curves of 13# specimen under different fatigue lives

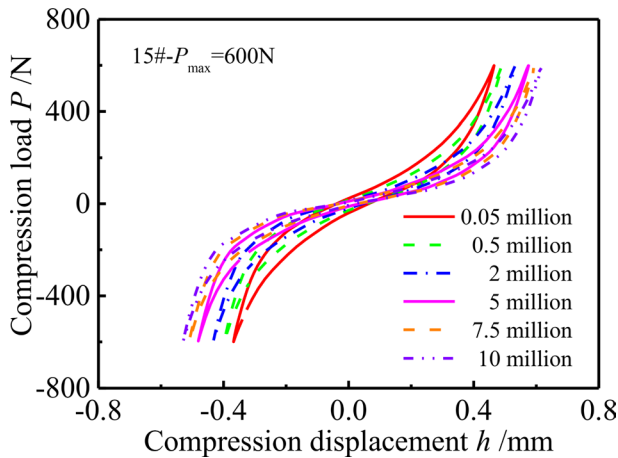


Fig. 8 Compression load-displacement hysteresis curves of 15# specimen under different fatigue lives

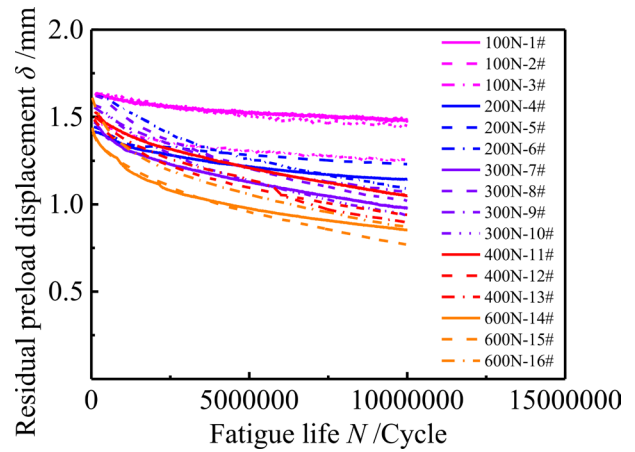


Fig. 9 Residual preload displacement versus fatigue life curves of metal vibration absorbers

assumed that the displacement amplitude of metal vibration absorber has no preload displacement change before reaching the minimum initial displacement amplitude, and then the residual preload displacement of metal vibration absorber decreases with the increase of the displacement amplitude. Based on the initial preload displacement of metal vibration absorber and the remaining preload displacement after 10 million cycles of fatigue test, the evolution of the preload displacement can be estimated by Eq. (3)

$$\frac{\delta_i - \delta}{\delta_i - \delta_f} = \frac{\nabla h}{\nabla h_{\max}} \quad (3)$$

where δ is the real-time residual preload displacement under any fatigue life, and δ_i is the initial preload displacement of metal vibration absorber. δ_f is the residual preload displacement measured after 10 million cycles of fatigue test. ∇h represents the change of displacement amplitude under the current fatigue life compared with the initial minimum displacement amplitude Δh_{\min} , namely $\nabla h = \Delta h - \Delta h_{\min}$. Analogously, ∇h_{\max} represents the change of displacement amplitude after 10 million fatigue lives compared with Δh_{\min} . Figure 9 shows the residual preload displacement versus fatigue life ($\delta-N$) curve of each metal vibration absorber. When the fatigue displacement amplitude of metal vibration absorber exceeds the residual preload displacement, there will be a large fatigue gap between the vibration absorber and the damping structure during the fatigue process, which may cause fatigue loosening. The damping effect of the metal vibration absorber will also decrease significantly at the same time. Consequently, it can be taken as the fatigue failure criterion when the fatigue displacement amplitude of metal vibration absorber is equal to its residual preload displacement, which shows a clear physical significance. Further, the failure life of vibration absorber can be obtained

after the test easily according to the fatigue failure criterion proposed in this paper. By comparing the displacement amplitude of each vibration absorber shown in Fig. 3 with the corresponding residual preload displacement shown in Fig. 9, it can be observed that only three samples with the maximum fatigue load of 600 N occur fatigue failure after 10 million cycles according to the failure criterion, and the critical fatigue lives of 14#-16# metal vibration absorbers are 3.65 million, 3.73 million and 5.79 million, respectively. Figure 10 shows the load-displacement hysteresis curves corresponding to the critical failure lives of the three metal vibration absorbers. It can be observed that the load-displacement hysteresis curves are relatively flat at this time, which represent the poor of energy absorption and vibration reduction effect. Therefore, it also confirms the validity of the residual preload displacement failure criterion. In conclusion, the residual preload displacement failure criterion is a macroscopical criterion, which is obviously superior to the initial preload displacement criterion or secant stiffness change rate criterion.

Since the increasing speed of the displacement amplitude decreases continuously during the process of the displacement amplitude of metal vibration absorber ranging from the initial minimum value to 10 million cycles of fatigue test (see Fig. 3). Similarly, the lowering speed of the residual preload displacement of metal vibration absorber also decreases continuously (see Fig. 9). Therefore, based on the variation ranges of displacement amplitude and preload displacement of each metal vibration absorber during the first 10 million cycles of fatigue test, it is assumed that the displacement amplitude and preload displacement of the vibration absorber will change the same results behind every 10 million cycles of fatigue test. Further, the fatigue

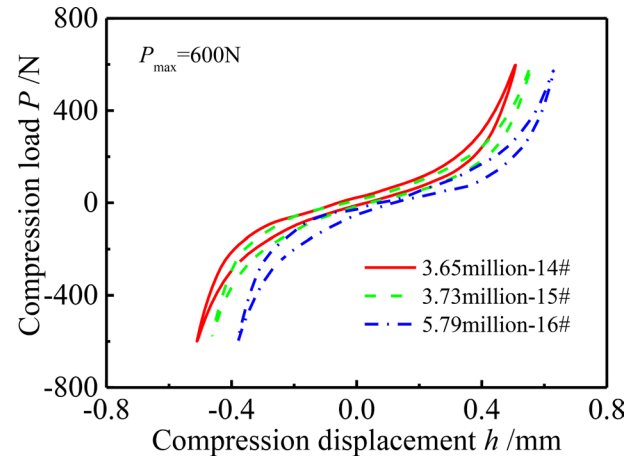


Fig. 10 Critical load-displacement hysteresis curves of metal vibration absorbers with maximum load of 600 N

failure life of each metal vibration absorber can be predicted when the displacement amplitude of the metal vibration absorber is equal to the residual preload displacement. Compared with the real fatigue life, this predicting life is a conservative result, which is more safety for engineering applications. The predicted fatigue lives of metal vibration absorbers according to the residual preload displacement failure criterion are listed in Table 2. And Fig. 11 shows the corresponding $P-N$ curve of metal vibration absorber based on the fatigue tests. It can be seen that the fatigue failure lives of metal vibration absorbers predicted by the residual preload displacement failure criterion show a good law of power function, which can be described as.

$$P_{\max} = 7340847.04N^{-0.6089} \quad (4)$$

Table 2 Fatigue life testing results of the metal vibration absorbers

Specimen number	Maximum load P_{\max}/N	Initial preload displacement δ_i/mm	Residual preload displacement δ_f/mm	Maximum secant stiffness $S_{\max}/N \cdot mm^{-1}$	Stiffness change rate $\lambda_{10m}/\%$	Predicted life $N/Cycle$
100 N-50 Hz-1#	100	1.635	1.480	2595.0	13.0	93,560,000
100-50 Hz-2#	100	1.620	1.450	2423.7	10.3	85,700,000
100 N-50 Hz-3#	100	1.470	1.245	2152.0	15.6	56,855,000
200-50 Hz-4#	200	1.415	1.145	1687.0	32.6	30,600,000
200-50 Hz-5#	200	1.445	1.230	1996.1	27.4	43,000,000
200 N-50 Hz-6#	200	1.610	1.090	2072.5	24.8	24,282,000
300 N-50HZ-7#	300	1.470	0.980	1561.3	30.6	16,300,000
300 N-50HZ-8#	300	1.620	1.020	1753.0	28.4	17,380,000
300 N-50HZ-9#	300	1.555	1.020	1980.5	31.4	18,560,000
300 N-50HZ-10#	300	1.565	0.940	1890.8	30.4	16,340,000
400 N-50HZ-11#	400	1.530	1.050	1619.5	28.3	15,310,000
400 N-50HZ-12#	400	1.485	0.940	2106.0	32.3	15,250,000
400 N-50HZ-13#	400	1.500	0.90	1652.5	33.6	12,025,000
600 N-50HZ-14#	600	1.440	0.855	1627.5	35.6	3,650,000
600 N-50HZ-15#	600	1.410	0.770	1439.9	27.4	3,730,000
600 N-50HZ-16#	600	1.610	0.870	1637.2	32.6	5,790,000

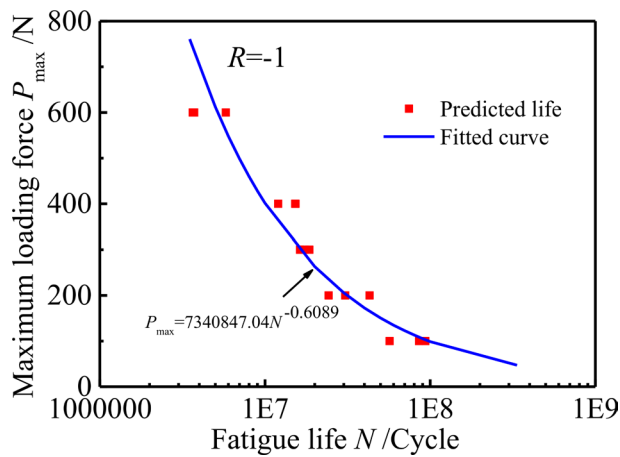


Fig. 11 P - N curve determined from the fatigue tests of metal vibration absorbers

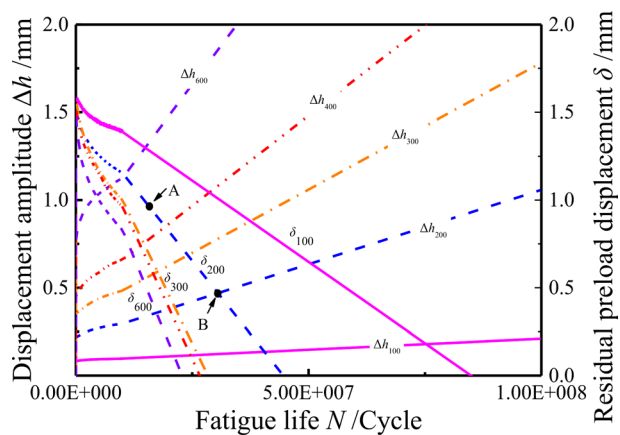


Fig. 12 Fatigue failure assessment diagram of the metal vibration absorber

The average curves of the displacement amplitude-life relations and residual preload displacement-life relations of the metal vibration absorbers under the same load levels can be obtained on the basis of the Figs. 3 and 9, respectively. And the predicted displacement amplitude and residual preload displacement under longer life can be determined by assuming that the displacement amplitude and preload displacement of the vibration absorber will change the same result behind every 10 million cycles of fatigue test. With reference to the classical J -integral crack driving force diagram of EPRI manual [22], a similar fatigue failure assessment diagram can be established to assess the fatigue life of the metal vibration absorber, as shown in Fig. 12. It can be seen that the average displacement amplitude-life curves and residual preload displacement-life curves of metal vibration absorbers under different load levels show certain laws, but the average residual preload displacement-life curves of metal vibration absorbers under the fatigue load of 300 N and 400 N are very close due to their own dispersions.

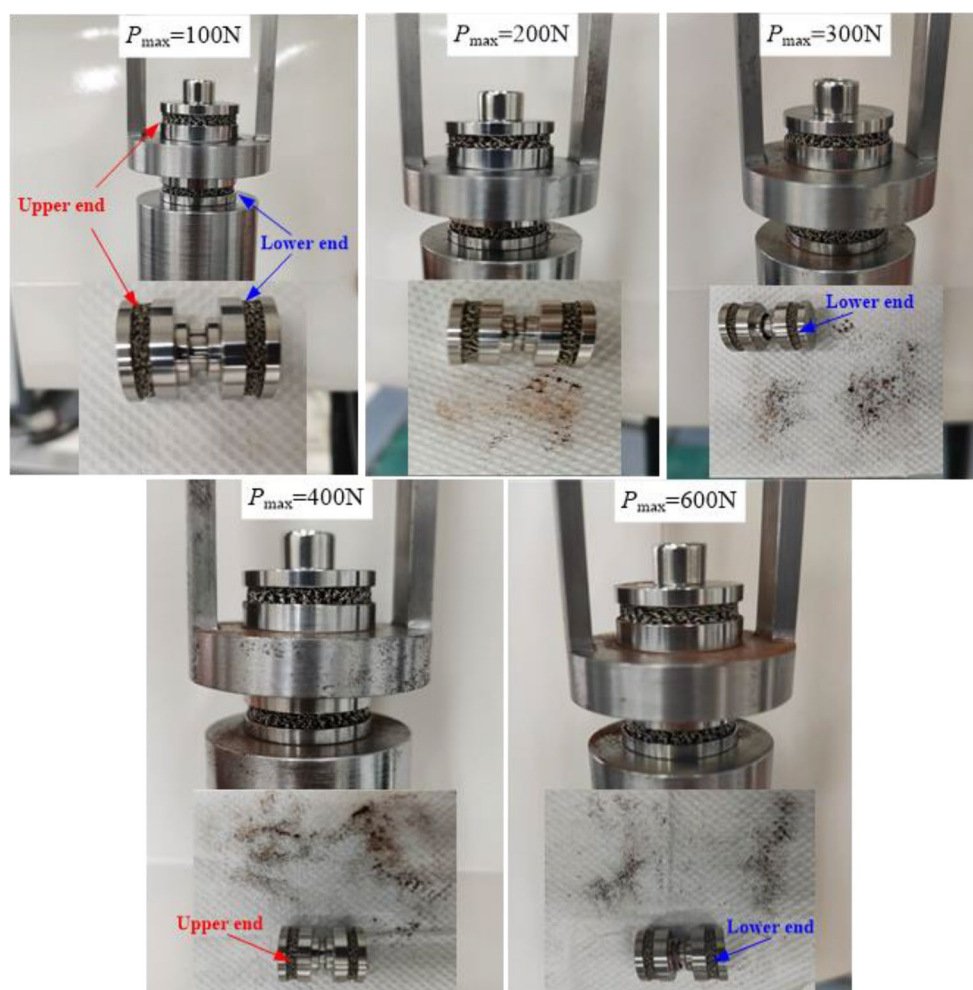
According to the failure criterion that the preload displacement is equal to the fatigue displacement amplitude, the failure life obtained when the fatigue load is 300 N is still significantly higher than that obtained when the fatigue load is 400 N. With the help of the fatigue failure assessment diagram, the residual fatigue life of the in-service metal vibration absorber can also be predicted. For example, if the load level and residual preload displacement of the in-service metal vibration absorber are assumed to be at point “A” in Fig. 12, and the corresponding in-service fatigue life is 2.1×10^7 . The average failure life of the fresh metal vibration absorber under the current load level is at point “B” in Fig. 12, the fatigue life of which is 3.05×10^7 . Therefore, the predicted residual fatigue life of the in-service metal vibration absorber is about 9.5×10^6 . For other service load levels that have not been tested, the displacement amplitude-life curves and residual preload displacement-life curves can be determined by interpolation method through the existing test data, so as to evaluate the failure life.

Fatigue Wear Analysis of Metal Vibration Absorber

Metal vibration absorber dissipate energy mainly through the friction of metal wire, which has obvious fatigue wear and slagging phenomenon. For some specific service environments, this slagging phenomenon may cause short circuit of electronic devices, which has certain safety risks. Because the phenomenon of metal wire slagging is difficult to be described quantitatively, some simple observations and analyses are carried out in this study. It is assumed that the metal wire component of metal vibration absorber close to the nut is called the upper end, and the metal wire component close to the lower fixture is called the lower end. The fatigue slagging phenomenon of metal vibration absorber after 10 million cycles is photographed in the test. Because the slags are mostly left inside the metal vibration absorber, manually shake off the residue of the metal vibration absorber on the white paper and take photos. Figure 13 shows the slagging photos of metal vibration absorbers under different fatigue load levels. It can be found that the friction slagging phenomenon of lower end of metal vibration absorber is more serious because of the higher constraint of lower end. When the fatigue load is less than 100 N, the slagging phenomenon can not be observed obviously after 10 million cycles of fatigue test. When the fatigue load is greater than 200 N, the obvious slagging phenomenon can be observed after 10 million cycles, and the larger the fatigue load is, the more obvious the slagging phenomenon is.

The fatigue wear condition of metal vibration absorbers is analyzed by means of scanning electron microscopy. Figure 14 shows the microscopic wear condition of metal vibration absorber after 10 million cycles under 200 N fatigue

Fig. 13 Pictures of the slagging phenomenon for metal vibration absorbers after 10 million cycles of fatigue tests



load. It can be observed that there is obvious wear debris on the local metal wire, but the metal wire fracture phenomenon does not appear in the metal wire component. Figure 15 shows the microscopic wear condition of the metal vibration absorber after 10 million cycles under 300 N fatigue load. The wear condition is significantly higher than that under 200 N fatigue load, and a fractured metal wire is found in the lower end metal wire component. Figure 16 shows the microscopic wear condition of the metal vibration absorber after 10 million cycles under 600 N fatigue load. A large number of wear slag and fracture phenomena of metal wires are observed in the metal vibration absorber. On the whole, the edge of the metal wire component near the center metal sheet is more likely to suffer from fatigue wear. The wear conditions of different parts of the metal wire component show obvious differences, which indicate that the carrying capacity of metal vibration absorber under different zones are also different. Moreover, the metal vibration absorber still has a good bearing capacity when some of the metal wires have broken, which only has a certain influence on the damping performance of the metal vibration absorber.

However, the failure ratio of HCF and wear is different to distinguish, which will be considered in the further research.

Three-Dimensional Tomography Analysis of Metal Vibration Absorber

Three-dimensional tomography (μ CT) equipment is adopted to conduct the microscopic analysis of the metal vibration absorber. Figure 17 demonstrates the μ CT picture of metal wire component in the new metal vibration absorber. It can be seen that the integrity of the metal wire component is good. The metal wire fracture phenomenon has not been found even changing the viewing angle, which represents that no metal wire fracture occurs in the process of integrated braid extrusion forming for metal wire component. In addition, it can also be observed that the deformation in the different parts of the metal wire after extrusion forming is unordered, resulting in a large dispersion of the performance of the vibration absorber. Metal wire volumes in different height regions of the two new metal wire components are analyzed by μ CT equipment, as shown in Table 3.

Fig. 14 SEM observed result of metal wire component with P_{\max} fixing at 200 N and N at 10 million



Fig. 15 SEM observed result of metal wire component with P_{\max} fixing at 300 N and N at 10 million

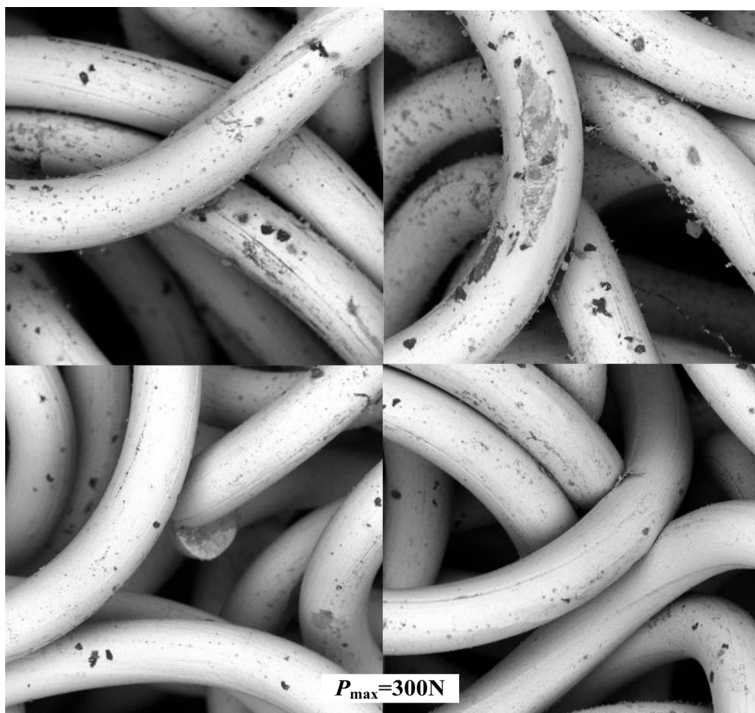
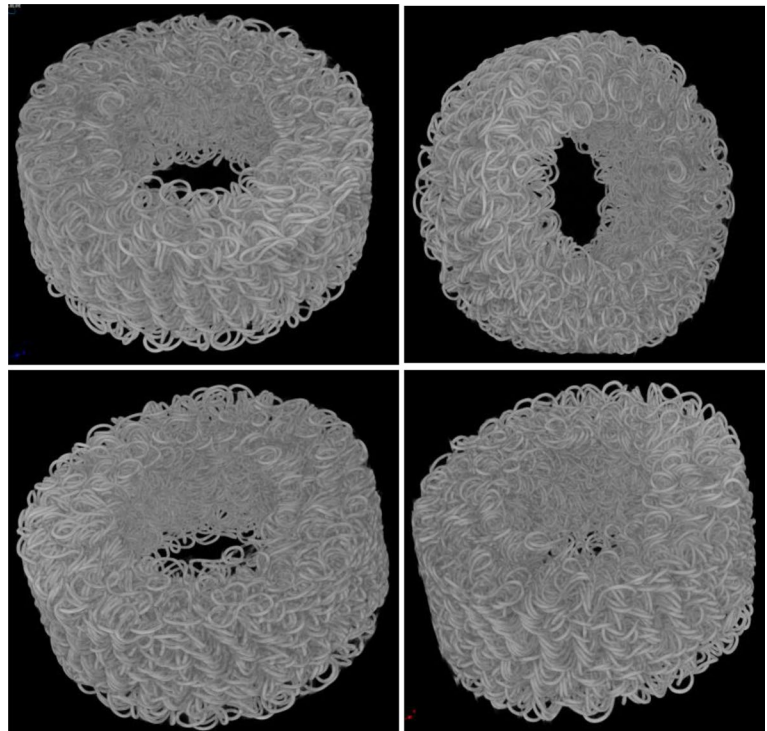


Fig. 16 SEM observed result of metal wire component with P_{\max} fixing at 600 N and N at 10 million



Fig. 17 Three-dimensional tomography picture of the new metal wire component



The results indicate that the volume contents of metal wire in different height regions of metal wire components show small deviations.

Figures 18, 19, 20 show the three-dimensional scanning pictures of the metal vibration absorbers after 10 million cycles under different fatigue loads, respectively. The results indicate that no metal wire fracture phenomenon is

found at the upper end of the metal wire components after 10 million cycles when the maximum fatigue load is 200 N and 300 N, but a small amount of metal wire fracture occurs on the top surface of the lower end metal wire component in contact with the central metal sheet, which also indicates that the metal wire wear at the lower end of the metal vibration absorber is more serious than that at the upper end.

Table 3 Metal wire volumes of the metal vibration absorbers in different height zones

Analysis height range	Component 1	Component 2
	Metal wire volume V / mm^3	Metal wire volume V / mm^3
(2~3.5)mm	101.1	95.46
(3.5~5)mm	103.0	101.2
(5~6.5)mm	101.1	99.46
(6.5~8)mm	93.49	95.97
Average value	99.68	98.03
Standard deviation	4.23	2.78

When the maximum fatigue load is 600 N, both the upper and lower ends of the metal wire components appear more metal wire fracture phenomena, and some metal wire fracture phenomena are also observed on the lateral of the metal wire component.

Conclusions

In this paper, the macro and micro approaches are adopted to research the fatigue properties of the metal vibration absorbers. Conclusions of the current study are given below:

- (1) Both the initial preload displacement and the secant stiffness change rate of the fatigue load-displacement hysteresis curve are not suitable for the fatigue failure

criterion of the metal vibration absorber. A new criterion is proposed to judge the fatigue failure of metal vibration absorber when the residual preload displacement of the metal vibration absorber is equal to the fatigue displacement amplitude;

- (2) The residual preload displacement prediction formula of metal vibration absorber is established. Further, a conservative fatigue failure life prediction method is put forward for the metal vibration absorber without fatigue failure. The experimental results demonstrate that the $P-N$ curve of the metal vibration absorbers predicted by the new method shows a good power function relation.
- (3) Based on the experimental displacement amplitude-life curves and the residual preload displacement-life curves of the metal vibration absorbers, a corresponding fatigue failure assessment diagram is drawn successfully. Then the residual fatigue failure life of in-service metal vibration absorber can be predicted according to the fatigue failure assessment diagram.
- (4) The microanalyses of the metal vibration absorbers are performed by means of the scanning electron microscopy and three-dimensional tomography equipment. The results indicate that the integrity of the metal vibration absorber is very good when it is produced, and no metal wire fracture phenomenon is observed. Moreover, the metal wire located in the upper edge of the lower end metal wire component near the central metal sheet is the most prone to occur fatigue wear and fracture phenomenon.

Fig. 18 Three-dimensional tomography picture of the metal wire component with P_{max} fixing at 200 N

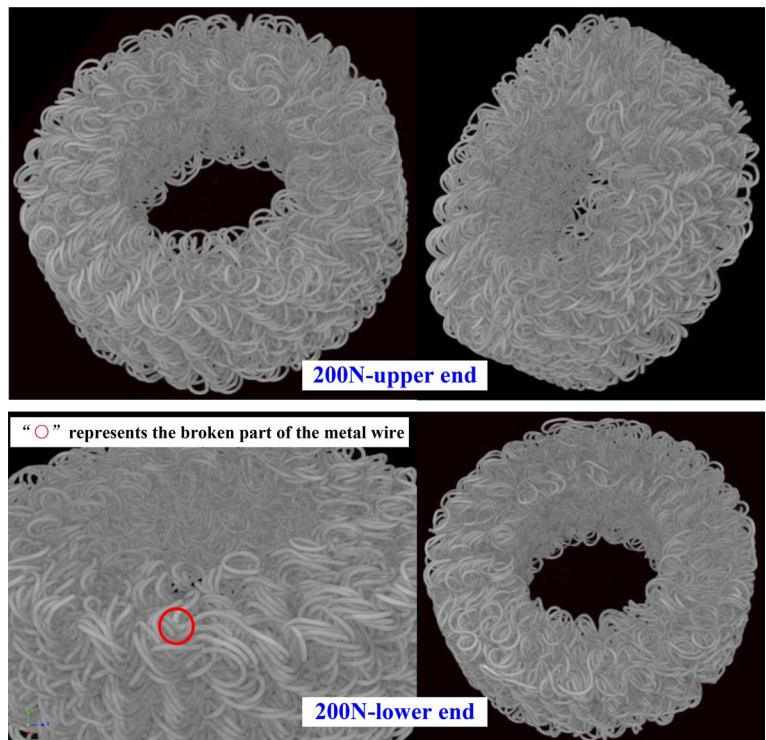


Fig. 19 Three-dimensional tomography picture of the metal wire component with P_{\max} fixing at 300 N

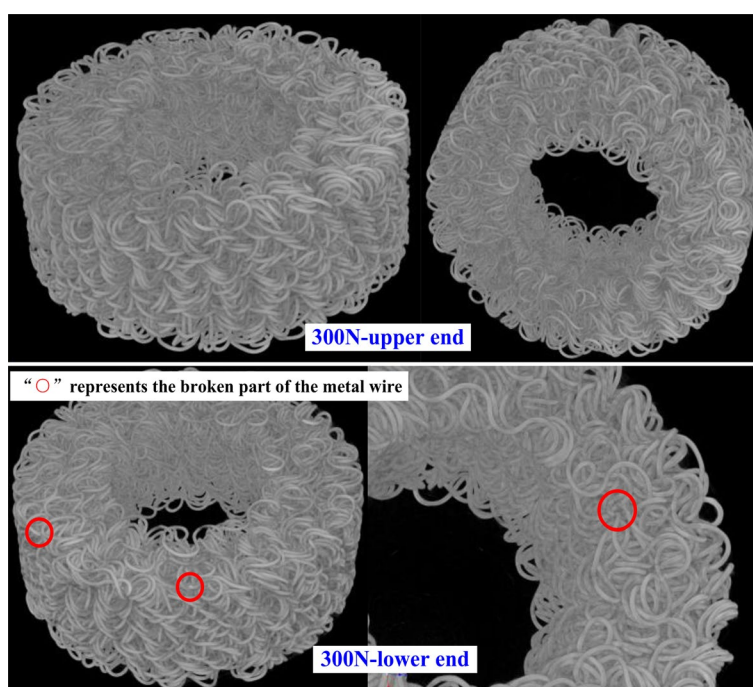
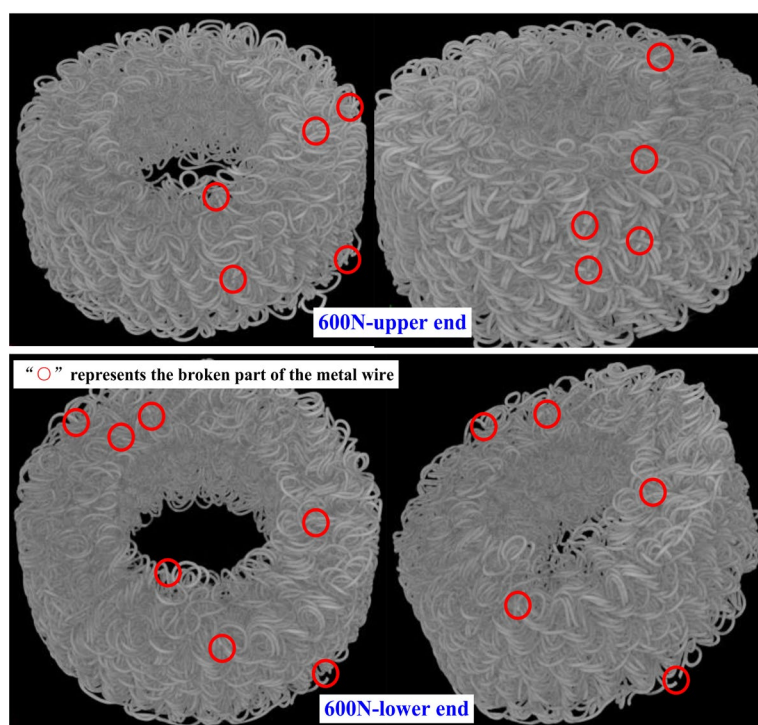


Fig. 20 Three-dimensional tomography picture of the metal wire component with P_{\max} fixing at 600 N



Consequently, this study put forward a novel fatigue failure criterion of metal vibration absorber. Further, a set of fatigue life prediction and evaluation method of the metal vibration absorber is successfully established, so as to realize the residual fatigue life prediction of the in-service metal vibration absorber. Moreover, the microscopic failure law of the metal vibration absorber under fatigue loading is also obtained.

Acknowledgements The authors gratefully acknowledge financial support from the national natural science foundation youth project of China (Grant no. is 12302108), the key projects of the national natural science foundation of China (Grant no. is 12172344) and the Sichuan natural science foundation outstanding youth science foundation project (Grant no. is 2023NSFSC1913). The authors thank the helpful comments and suggestions from anonymous reviewers.

Author Contributions PYQ: Investigation, Methodology, Writing—original draft. JD: Software, Experiment, Validation. CZ: Microanalysis. GY: Fixture processing. ZWZ: Writing—review & editing, Fund-

ing acquisition, Project administration.

Data Availability Data available on request.

Declarations

Consent for Publication All authors approved the final manuscript and submission to the journal.

Competing Interests The authors declare that they have no known competing financial interests or personal relationships that could have appeared to influence the work reported in this paper.

Human and Animal Rights No animal or human subjects were used in this research.

References

- Ulanov AM, Lazutkin GV (1997) Description of an arbitrary multi-axial loading process for non-linear vibration isolators[J]. *J Sound Vib* 203(5):903–907
- Ertas BH, Luo H (2007) Nonlinear dynamic characterization of oil-free wire mesh Dampers[J]. *J Eng Gas Turbines Power* 130(3):1225–1234
- Ertas BH (2009) Compliant hybrid Journal Bearings using integral wire mesh Dampers[J]. *J Eng Gas Turbines Power* 131(2):1215–1226
- Andrés LS, Chirathadam TA (2011) Metal Mesh Foil Bearing: Effect of Motion Amplitude, Rotor Speed, Static load, and excitation frequency on Force Coefficients[J]. *J Eng Gas Turbines Power* 133(12):1201–1228
- Westergaard RH, York OH Elastic metal mesh tubular bellows: US2755079[P]. 1956-07-17.
- CREDE C E Vibration isolator: US2610016[P]. 1952-09-09
- Zhang DY, Xia Y, Zhang QC et al (2018) Researches on metal rubber mechanics properties in retrospect and prospect[J]. *J Aerosp Power* 33(6):1432–1445 (in Chinese)
- Zhang DY, Scarpa F, Ma YH et al (2014) Dynamic mechanical behavior of nickel-based superalloy metal rubber[J]. *Mater Design* 56(1):69–77
- Ma Y, Zhang Q, Zhang D et al (2014) A novel smart rotor support with shape memory alloy metal rubber for high temperatures and variable amplitude vibrations[J]. *Smart Mater Struct* 23(12):116–123
- Lin Y, Zhang Z, Ren Z et al (2021) A solvent-responsive robust superwetting titanium dioxide-based metal rubber for oil-water separation and dye degradation[J]. *Colloids Surf Physicochemical Eng Aspects* 614:126–136
- Lu ZR (2005) Research on combined stiffness characteristic of metal rubber damper[D]. Harbin Institute of Technology. (in Chinese)
- Hao HR, Bai HB, Zhang HJ (2009) Comparison of damping capacities between non-circular section wire metal rubber and ordinary metal rubber[J]. *Mech Sci Technol Aerosp Eng* 28(2):210–213 (in Chinese)
- Hu JL, Du Q, Gao JH et al (2018) Compressive mechanical behavior of multiple wire metal rubber[J]. *Mater Design* 140:231–240
- Huang K, Bai HB, Lu CH et al (2016) Rare metal Mater Eng 45(3):681–687 (in Chinese). Numerical Simulation of Metal Rubber Press Forming[J]
- Zhang DY, SCARPA F, Ma Y et al (2013) Compression mechanics of nickel-based superalloy metal rubber[J]. *Mater Sci Engineering: A* 580(37):305–312
- Bin Z, Yanhong M, Dayi Z et al (2012) A constitutive model of metal rubber based on hysteresis property. *Acta Phys Sinica* 61(7):191–197
- Ma Y, Di G, Zhang D et al (2015) Compressive and dissipative behavior of metal rubber under constraints[J]. *Phys Status Solidi (b)* 252(7):1675–1681
- Jiang H, Xia Y, Ao H et al (2005) Life time of metal rubber isolator with different vibration amplitudes[J]. *J Cent South Univ Technol* 12(2):181–185
- Ao HR, Jiang HY, Ulanov AM (2006) Estimation of the Fatigue Lifetime of Metal Rubber Isolator with Dry Friction Damping[J]. *Key Eng Mater*, 326–328: 949–952
- Li Y (2019) Experimental study on fatigue life of metal-net Rubber Damper[D]. Harbin Institute of Technology. (in Chinese)
- Cao FL, Bai HB, Yang JC et al (2012) Analysis on fatigue damage of Metal Rubber Vibration Isolator[J]. *Adv Mater Res*, 490–495: 162–166
- Kumar V, German MD, Shih CF (1981) Engineering approach for elastic-plastic fracture analysis. Electric Power Research Institute. EPRI Report NP-1931

Publisher's Note Springer Nature remains neutral with regard to jurisdictional claims in published maps and institutional affiliations.

Springer Nature or its licensor (e.g. a society or other partner) holds exclusive rights to this article under a publishing agreement with the author(s) or other rightsholder(s); author self-archiving of the accepted manuscript version of this article is solely governed by the terms of such publishing agreement and applicable law.